

Artificial intelligence-enhanced DTC command methods used for a four-wheel-drive system

Ndoubé Matéké Max¹, Njock Batake Emmanuel Eric¹, Nyobe Yomé Jean Maurice¹,
Mouné Cédric Jordan¹, Manyol Moise¹, Olong Georges¹, Alain Biboum²

¹Energy, Materials, Modelling and Methods Research Laboratory (LE3M), National Higher Polytechnic School of Douala,
University of Douala, Douala, Cameroon

²Mechanical and Industrial Engineering Department, National Advanced School of Engineering of Yaoundé, University of Yaoundé I,
Yaoundé, Cameroon

Article Info

Article history:

Received Apr 4, 2023

Revised Jun 9, 2023

Accepted Jun 25, 2023

Keywords:

Artificial intelligence

Direct torque control

Electric vehicle

Induction motor

Variable master slave control

ABSTRACT

This paper presents an artificial intelligence direct torque control (DTC) method for an electric vehicle (EV) drive system. The architecture of the proposed electric vehicle is that of four wheels each with an induction motor (IM). A comparative study of the different torque and speed controllers proposed in this paper is made. An electronic differential is used to control the speed of each wheel as well as a variable master-slave control (VMSC) for the management of the magnetic quantities because the motors on the same side are fed by the same converter. This study allows highlights the performance of the propulsion system in terms of dynamics and safety of the vehicle and better stability. The different controllers are implemented by the MATLAB/Simulink software and the simulation results obtained show better flexibility in the control of the vehicle. It is worth noting that direct torque control with fuzzy logic (DTFC) performs better than DTC associated with neural networks in terms of a time reduction increase of 1.47%, an overshoot of less than 5.33, and a static steady-state error close to zero.

This is an open access article under the [CC BY-SA](#) license.



Corresponding Author:

Ndoubé Matéké Max

Energy, Materials, Modelling and Methods Research Laboratory (LE3M), National Higher Polytechnic
School of Douala, University of Douala

Carrefour Ange Raphaël, Douala, Cameroon

Email: mdesmax@yahoo.fr

1. INTRODUCTION

There is no doubt that the preservation of the environment is a necessity given almost irreversible harmful climatic changes caused, among other things, by pollution due to the emission of greenhouse gases [1], [2]. Among the currently recommended solutions, the development of the electric vehicle (EV) is found. It must progressively replace the internal combustion engine vehicle. The related research and development programs are being implemented by the States (USA, China, India) [3] and the major automobile industries. The current automotive market has three variants [3], internal combustion vehicles, hybrid vehicles, and electric vehicles. The motive power of the EV is based on the electric actuator that provides its drive. The choice of the propulsion machine and its control strategy play a key role from a technical and economic point of view (ease of manufacture of equipment, cost reduction, reduction of torque and flow oscillations, solidity

in the face of road constraints) [4]. Induction motors are chosen as propulsion motors because of their higher efficiency, and low maintenance [4], [5]. These motors can only work optimally if they are driven by a proper control strategy such as direct torque control (DTC) [6].

EVs are gaining popularity due to their quiet, smooth, and emission-free operation, as well as their safety benefits, portable charging system, and improved fuel economy [7]. However, these vehicles have challenges such as excessive charging time and low energy density, which provide possible research areas for their improvement. These limitations can be overcome by implementing an effective control strategy. At this level, in modern research, the integration of artificial intelligence (AI) has gained importance due to the need to select the most appropriate parameters, allowing the most efficient results [8], [9].

Thus in [10], a review of several direct torque control (DTC) schemes associated with fuzzy logic (FL), artificial neural networks (ANN), sliding mode control (CMG), and genetic algorithms (GA) were presented to improve the performance of an induction motor (IM). A comparison was made between these control systems in terms of algorithm complexity, parameter sensitivity, ripple reduction, switching loss, and speed tracking. The authors concluded that it was very difficult to choose an appropriate control scheme because it depended on the application, accuracy, hardware availability, reliability, and system cost. An ANN-based DTC scheme was introduced for an electric vehicle powered by a fuel cell [11]. This scheme used the flux of the stator as a control variable and the flux level was adjusted according to the torque demand of the EV to achieve high drive performance. In this paper, the authors examined the performance of an IM drive for EV propulsion without considering the actual vehicle dynamics (road load), range, and fuel economy.

Thus in [12], an improved direct instantaneous torque control (DITC) based on adaptive terminal sliding mode control (ATSMC) was proposed. This is a new DTC technique for motors. A DTC scheme based on a stator flux optimization algorithm to increase the range of an electric vehicle in terms of driving a 3 kW induction motor at full load is tested by considering the effect of core losses and leakage inductance as explain in [13]. Araria *et al.* [14] presented a DTC scheme for a battery and fuel cell-powered front-wheel-drive EV with an ANN speed PI controller allows for accurate reference speed tracking compared to traditional PI controllers using standard driving cycles such as the US environmental protection agency (EPA) and the new European driving cycle (NCCE). A comparative study between ANN and GA is done on an EV propulsion system to examine the torque setting, EV behavior in terms of range, speed, and fuel efficiency as elaborated in [7]. An evaluation of the percentage of charge rate and the energy consumption are made under various road conditions.

This study proposes to evaluate two direct torque control (DTC) methods combined with artificial intelligence for a four-wheel-drive system of an electric vehicle. A comparison is made between fuzzy logic (FL) and artificial neural network (ANN) tuning. Both algorithms are used to adjust the error of the electromagnetic torque and magnetic flux to reduce the magnitude of their ripples. The proposed propulsion system was tested on the standard worldwide harmonized light vehicles test procedure (WLTP) driving cycle and performance parameters such as range and fuel efficiency were evaluated. The responses of the two intelligent algorithms are observed in terms of algorithm complexity, torque and flow ripple, control efficiency, improved flexibility, speed tracking, and ease of implementation. The performance obtained by the simulations indicates their adaptability to the use of such a propulsion system.

2. SYSTEM DESCRIPTION AND MODELLING

2.1. EV dynamics

The architecture of the EV developed in this paper is a twin-engine EV as shown in Figure 1. It contains key components of the conventional EV. Dynamics of vehicle are described by yaw rate, and speed both longitudinal and lateral as (1)-(3) [15], [16]:

$$v_x = v_y r + \frac{F_{t1} + F_{t2} + F_{t3} + F_{t4} - F_{tot}}{M_v} + \frac{C_f \delta}{M_v} \left(\frac{v_y + r l_r}{v_x} - \delta \right) \quad (1)$$

$$v_y = \left(-\frac{C_r + C_f}{M_v v_x} \right) v_y + \left(\frac{C_r l_r + C_f l_f}{M_v v_x} - v_x \right) r + \frac{C_f}{M_v} \delta \quad (2)$$

$$r = \left(\frac{C_r l_r - C_f l_f}{J_v v_x} \right) v_y - \left(\frac{C_r l_r^2 - C_f l_f^2}{J_v} \right) r + \frac{C_f l_f}{J_v} \delta + \frac{d}{J_v} (F_{t1} + F_{t2} - F_{t3} - F_{t4}) \quad (3)$$

When analyzing Figure 2 presented, different forces applied to the vehicle are mentioned for a better understanding. Then, in (4) indicating the EV resistance opposes to any movement can be easily carried out. Following forces, the tire rolling resistance F_{rr} , aerodynamic resistance in drag F_{wind} , levelling resistance F_g

and acceleration resistance F_l are needed for a calculation of the required total force all these resistances are discussed detailly in [17]–[19].

$$F_t = F_{rr} + F_{wind} + F_g + F_l \quad (4)$$

Where:

$$F_{rr} = gMv \cos \alpha \quad (5)$$

$$F_{wind} = 0,5\rho S_f C_{px}(V_h - V_{air})^2 \quad (6)$$

$$F_g = gM_v \sin \alpha \quad (7)$$

$$F_l = \gamma M_v \quad (8)$$

The longitudinal forces of four-wheel motors can be calculated using as (9) [20].

$$F_{ti} = \frac{\delta M_v}{4} \mu_i \cos(\alpha_p), i \in [1, \dots, 4] \quad (9)$$

The model of drive system can be described as (10) and (11) [20],

$$T_{ri} = F_{ti} R_\omega - N_f d_z, i \in [1, 3] \quad (10)$$

$$T_{ri} = F_{ti} R_\omega - N_r d_z, i \in [2, 4] \quad (11)$$

where T_{ri} is the resistive couple; N_f, N_r , are normal front and rear forces calculated using as (12) and (13) [20]:

$$N_f = \frac{gM_v}{2} \left(\frac{l_r}{L} - \frac{h_{cg}}{L_g} * \frac{dv_{cg}}{dt} \alpha_p - \frac{h_{cg}}{L} \alpha_p \right) \quad (12)$$

$$N_r = \frac{gM_v}{2} \left(\frac{l_r}{L} + \frac{h_{cg}}{L_g} * \frac{dv_{cg}}{dt} \alpha_p + \frac{h_{cg}}{L} \alpha_p \right) \quad (13)$$

with a linear tire model, front and rear cornering forces can be expressed as the product of the cornering stiffness. (C_f, C_r) and sideslip angle (α_f, α_r) [20].

$$F_{yf} = -C_f \alpha_f \quad (14)$$

$$F_{yr} = -C_r \alpha_r \quad (15)$$

Sideslip angles of the wheels are expressed using the side length and angular speeds, as well as the steering angle δ . The explicit expressions of sideslip angles for front and rear axles are represented by (16) and (17) [20].

$$\alpha_f = \tan^{-1} \left(\frac{v_y + l_f r}{v_x} \right) - \delta \quad (16)$$

$$\alpha_r = \tan^{-1} \left(\frac{v_y - l_r r}{v_x} \right) \quad (17)$$

The longitudinal slip needs to be determined for all four wheels as (18):

$$\lambda_i = \frac{R_\omega \omega_i - u_{ti}}{\max(R_\omega \omega_i - u_{ti})}, i \in [1, \dots, 4] \quad (18)$$

where: $i = 1, 2, 3$ and 4 correspond to front left, front right, rear left and rear right ($=lf, fr, rl, rr$) wheels, respectively; R_ω is the radius of wheel; ω_i is the angular speed of motor in the wheel, and V is the linear speed at which the contact zone moves on the ground. Inter relationships between slip ratio λ and the traction coefficient μ can be described by various formulas. In this study, the widely adopted magic formula [21], [22], is applied to describe relationship between sliding and tensile forces in order to build a vehicle model in which following simulations are indicated by (19) [23], [24].

$$\mu = C_1 \left[\sin \left(C_2 \tan^{-1} \left(C_3 \lambda - C_4 (C_3 \lambda - \tan^{-1}(C_3 \lambda)) \right) \right) \right] \quad (19)$$

The sets of coefficients of C1, C2, C3 and C4 are defined in [25], [26]

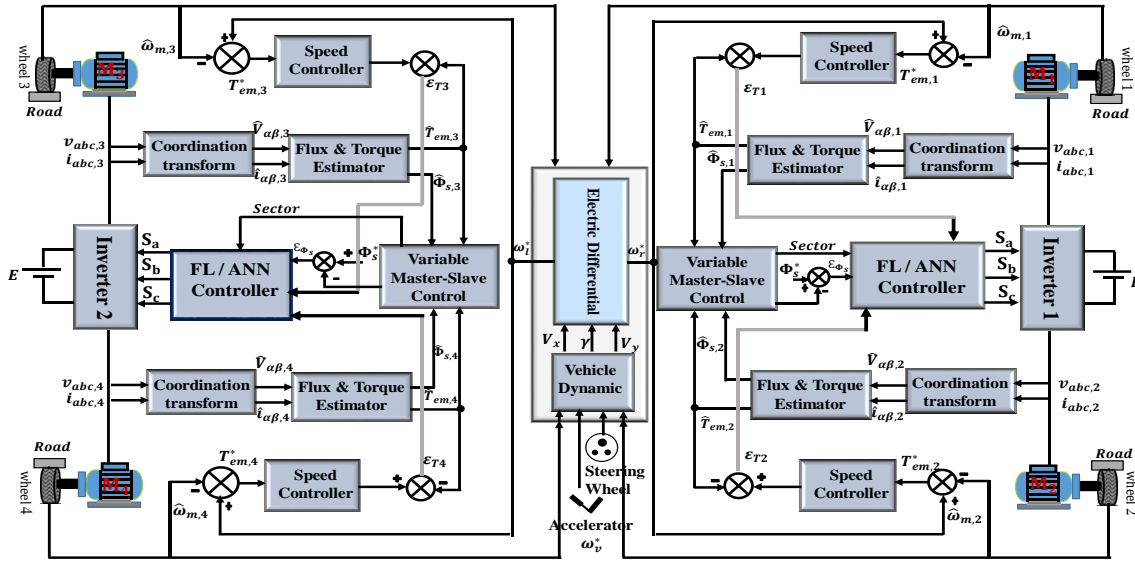


Figure 1. Architecture of the EV under investigation

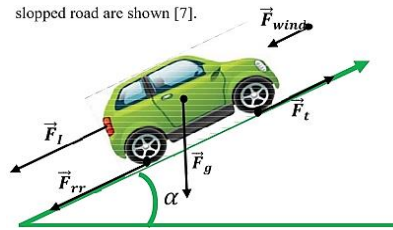


Figure 2. Forces on the vehicle [19]

2.2. Modeling of the electronic differential (ED)

The ED allows the management of the driving wheel speeds of the EV. On a straight path, it maintains the two speeds of the driving wheels at the same value. And for a curvilinear trajectory, depending on whether we are going left or right, it allows the speed of the wheel at the outside position of the curve to be greater. This prevents the tires from losing traction [4]. Figure 3 shows a sketch of an electronic differential used in EV modeling. The notations L_w , d_w and δ represent the wheelbase, the distance between driving wheels and the steering angle, respectively. The speeds ω_R^* and ω_L^* are the drive speeds of right and left motors. So when: $\delta > 0 \rightarrow$ Turn right, $\delta = 0 \rightarrow$ Straight ahead, and $\delta < 0 \rightarrow$ Turn left

It is possible to determine the reference speeds in relation to the driver's requirements. When vehicle arrives at the start of a path, the driver applies a steering angle on its wheel [21], [27]. The ED acts instantly on both motors, reducing the speed of the wheel drive located at the inside position of the curve, thus increasing the speed of the driving wheel outside the curve. The angular speeds of the driving wheels are given by the relations:

$$\omega_R^* = \left(\frac{V_h}{R_\omega} - \frac{\Delta\omega}{2} \right) \quad (20)$$

$$\omega_L^* = \left(\frac{V_h}{R_\omega} + \frac{\Delta\omega}{2} \right) \quad (21)$$

The difference between the angular speeds of the driving wheels can be expressed by (22) [8], [28]:

$$\Delta\omega = \frac{d_w \tan(\delta)}{L_w} \cdot \frac{V_h}{R_\omega} \quad (22)$$

with $L_w = L_f + L_r$

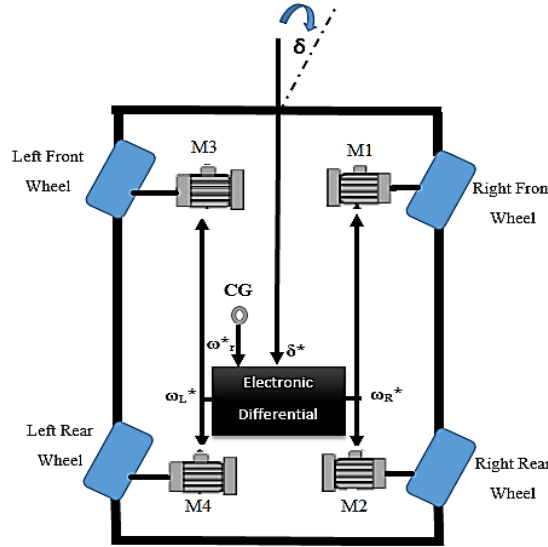


Figure 3. Structure of the electronic differential [4], [27]

2.3. Variable master slave control (VMSC)

This is a switchable master-slave control strategy. In this system, it makes it possible to regulate the stator flux of machines placed in parallel. This is because the power to these machines is provided by a single converter, and it may happen that these machines do not undergo the same loads. This implies that the functioning of some can hamper that of others (for example, the magnetic circuit of one machine can become saturated without that of the other). To avoid this, a means must be found so that voltage vectors delivered by the converter supply each machine equitably by enabling it to develop speeds and torques which are respectively required of them. In this case, it is a matter of regulating the stator flux of one machine at a time. This machine will be called master and thus makes the other a slave. While the stator flux of the master machine is controlled, that of the slave machine evolves naturally without respecting the set point so as to avoid saturation. The master machine is the one with the lowest torque. We, therefore, observe that when the torque of a machine increases, its stator flux decreases and vice versa.

3. ARTIFICIAL INTELLIGENCE BASED DTC DEVELOPMENT

3.1. Direct torque control by artificial neural networks (DTNC)

The DTNC control for multi-machine systems is shown in the Figure 4. The inputs that provide the network are: e_{Tem1} ; e_{Tem2} (error between the torques developed by the motors and the corresponding references); e_ϕ (error between the modulus of the stator flux and the fixed reference) and θ_s (position of the stator flux vector in the complex plane (α, β)). And the outputs are the pulses Sa; Sb; Sc necessary to drive the converter allowing to feed the motors adequately. During the training of the network with the data provided by the simulation of the conventional DTC control, when data is presented at the input of the network, the output is obtained by a calculation propagated from the input layer to the output layer. The calculation of the quadratic sum of the errors is obtained by (23):

$$E(k) = \frac{1}{N} \sum_{i=1}^N (d_i(k) - y_i(k))^2 \quad (23)$$

with: d_i the desired output; y_i the computed output; k the number of iterations and N the amount of data in the training database. And so, according to the method of retro propagation of the error, the error is propagated from the output to the inputs causing a modification of the synaptic coefficients of the network according to as (24):

$$w_{ji}(k+1) = w_{ji}(k) - \eta \frac{\partial E(k)}{\partial w_{ji}(k)} \quad (24)$$

with: w_{ji} the weight of the connection between the j -th neuron and the i -th neuron of the previous layer and η the learning constant. The network studies have the following characteristics:

- 4 layers, including 2 hidden layers each composed of 10 neurons. The input and output layers are composed of 3 neurons each.

- The activation functions used are linear (purelin) for the input and output layers and sigmoid (logsig) for the hidden layers.
- This is supervised learning, and the chosen learning algorithm is the backpropagation of error.
- The chosen optimization method is the Levenberg-Marquardt method for its speed and convergence.

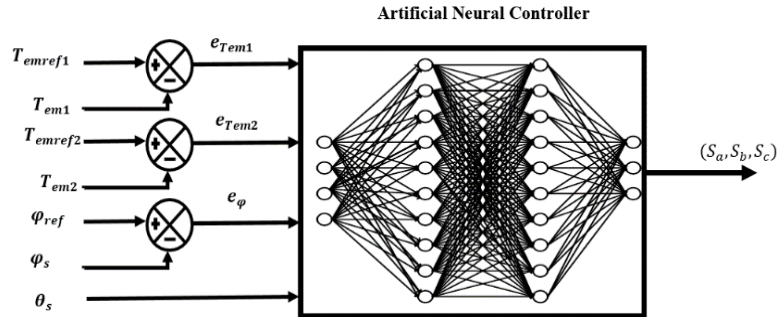


Figure 4. Neural controller structure for multi-machine system

3.2. Direct torque control with fuzzy logic (DTFC)

The second technique proposed in this article is the DTC associated with fuzzy logic. The block diagram of this command (DTFC) for a multi-machine system is shown in Figure 1 above. The fuzzy regulator includes 4 inputs which are:

- e_ϕ : Difference between the reference stator flux and the estimated stator flux.
- e_{Tem1} : Difference between the reference torque and the electromagnetic torque of motor 1.
- e_{Tem2} : Difference between the reference torque and the electromagnetic torque of motor 2.
- θ_s : Position du vecteur de flux statorique.

The stake around the control for multi-machine systems with one converter is to ensure the optimal functioning of the actuators in parallel. Indeed, it must be ensured that the converter provides an adequate voltage vector to meet the demands of the machines. Thus, just like the conventional DTC command applied to this type of system, the DTFC command comprises in its structure a control loop as shown Figure 5 of an electromagnetic torque regulation based on a Mamdani type fuzzy regulator.

Thus, it includes two inputs: $e_{Tem1} = T_{emRef1} - T_{em1}^*$ for motor 1 and $e_{Tem2} = T_{emRef2} - T_{em2}^*$ for motor 2 and an exit e_{Tem} . The universe of discourses for each set is represented is being as: For e_ϕ we have: N (negative) and P (positive); and For e_{Tem1} , e_{Tem2} we have: N (negative), Z (zero), and P (positive).

Trapezoidal and triangular membership functions were chosen. The torque error entry is made up of three fuzzy sets: N (negative), Z (zero) and P (positive) as shown in Figure 6 as shown in. This fuzzy regulator is governed by all the rules set out as shown in Table 1.

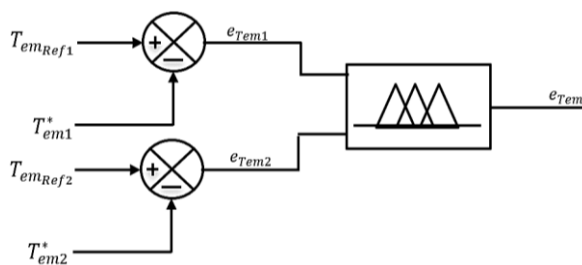


Figure 5. Structure of a fuzzy regulator for a multi-machine system

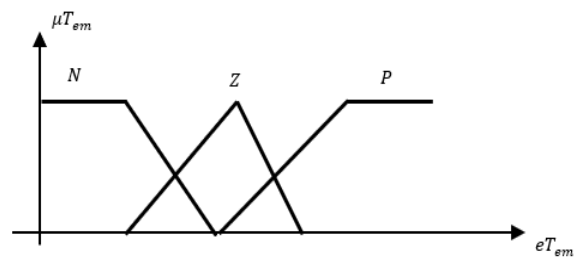


Figure 6. Membership function of torque error

Table 1. Basis of adopted rules

e_{Tem2}	e_{Tem1}		
	P	Z	N
P	P	P	Z
Z	P	Z	N
N	N	N	N

The output obtained will be used for the selection of the adequate voltage vector by another fuzzy regulator with as other inputs: i) The stator flux error; and ii) The position of the stator flux vector θ_s . The position of the stator flux vector is subdivided into six sectors. And for the outputs, the pulse signals used for the selection of the voltage vectors by the inverter are S_a , S_b , and S_c [20]. Thus, the rules obtained for the new method proposed can be deduced from the principle previously illustrated in the Table 1.

4. SIMULATION AND RESULT ANALYSIS

The simulation parameters used in this paper were chosen after an investigation in the literature. They come from the papers of [28], [29] with prototyping but also the papers [20], [27]. Table 2 gives the information of the path traveled by the vehicle. The vehicle leaves the stop state to reach the speed of 70 km/h at $t = 2$ s. The driver maintains this speed until $t = 4$ s. Between $t = 4$ s and $t = 9.5$ s the vehicle negotiates a right turn with a steering command of 7° is shown in Figure 7 and a speed of 50 km/h. Back on a straight line between $t = 9.5$ s and $t = 12$ s the vehicle is driving at 70 km/h. Left turn with a stabilized speed of 50 km/h between $t = 12$ s and $t = 17.5$ s. Then the Vehicle faces a slope of 10% until $t = 19$ s maintaining a speed of 40 km/h, then returns to a straight road for the rest of the trip at a speed of 50 km/h as shown in Figure 8. Thus, the chosen speed profile allows the vehicle to cover a distance of 290 m in the 20s as shown in Figure 9. Figure 10 allows us to appreciate the action of the electronic differential during the turns, the engines of the right side slower when the turn is on the right contrary to the engines of the left and vice versa. This is explained by the fact that the wheels on the inside of the curve support a significant weight of the vehicle moving towards the inside.

During the start [0s; 2s], the 04 motors that compose the system develop a very important torque to allow the vehicle to overcome the inertia and reach the speed wanted by the driver. During the turns [4s; 9.5s] and [12s; 17.5s], the torques of the motors located inside the turn increase to allow the wheels to keep the desired speed while supporting the weight of the vehicle which moves on their side, the motors located on the opposite side are driven which explains that the developed torques are of negative sign as shown in Figure 11. For conventional direct torque control, oscillations are significant and go beyond the set hysteresis range [-0.5N.m; 0.5N.m]. Figures 11(a) and 11(b) illustrate the contribution of artificial intelligence control techniques in reducing these oscillations, with DTFC offering the best result.

Table 2. Chronology of the journey made by the EV

Phases	Time (s)	Road information	Vehicle speed (Km/h)	Phases	Time (s)	Road information	Vehicle speed (Km/h)
01	0s < t < 2s	Starting the vehicle	70	05	12s < t < 17.5s	Left turn	50
02	2s < t < 4s	Flat and straight road	70	06	17.5s < t < 19s	10% slope	40
03	4s < t < 9.5s	Right turn	50	07	19s < t < 20s	Flat and straight road	50
04	9.5s < t < 12s	Flat and straight road	70				

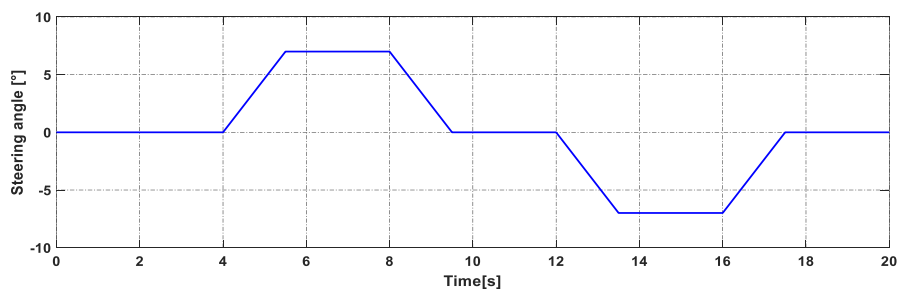


Figure 7. Steering angle variation

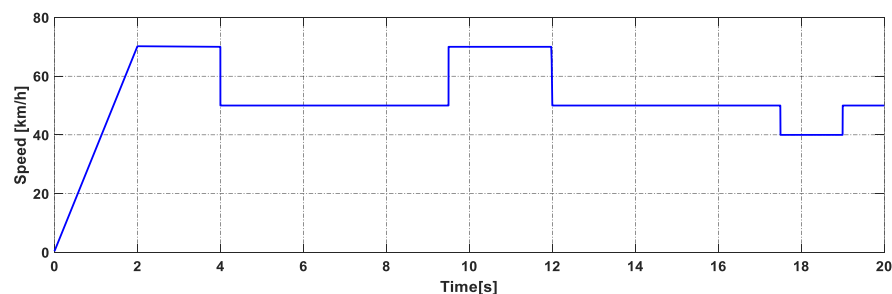


Figure 8. Speed profile

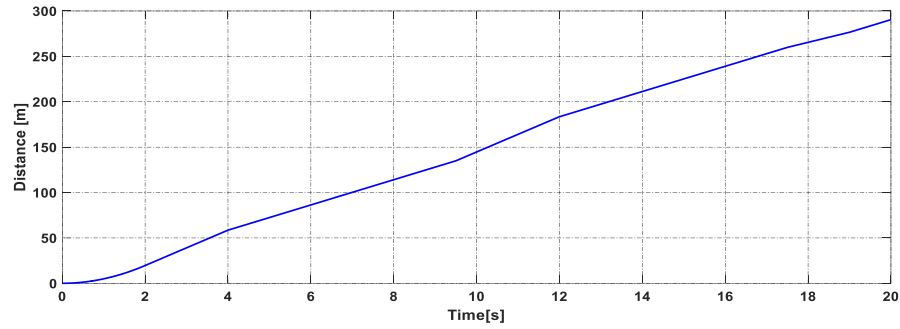


Figure 9. Distance traveled

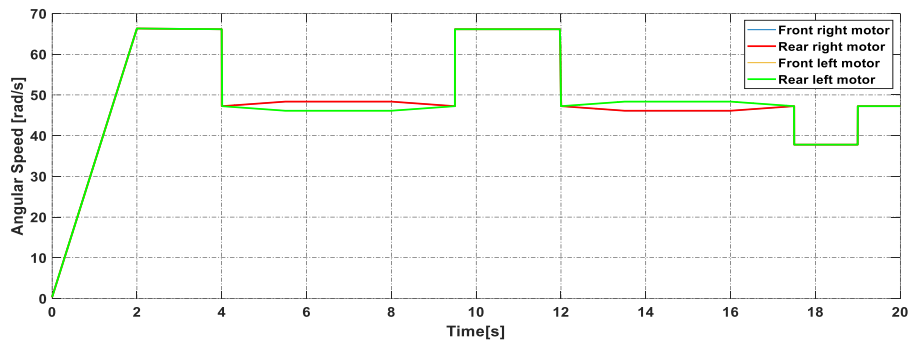


Figure 10. Angular velocity references

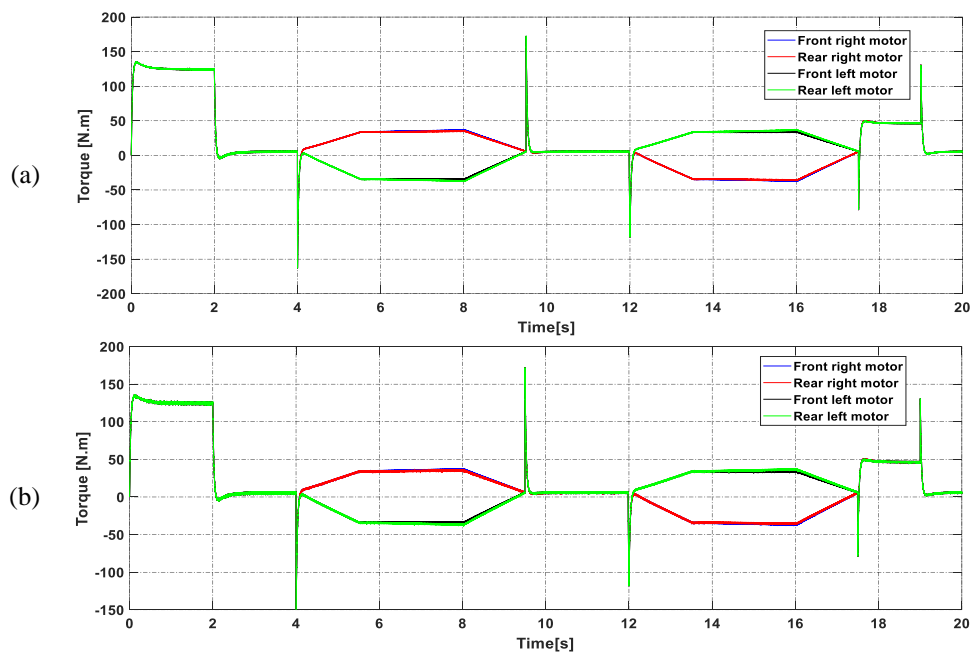


Figure 11. Electromagnetic torque (a) DTFC and (b) DTNC

Motor speed response is better for DTFC control than for the other two strategies, as shown in Figure 12. Figure 12(a) shows the evolution of the speed curves derived from artificial intelligence and conventional vehicle control. Figure 12(b) shows the system's performance in terms of response. Table 3 shows some performance values.

Overall, the direct torque control strategy ensures good engine and vehicle control. Moreover, the results show the compatibility of this control for an application to multi-machines/mono converter systems,

which added to an energy-saving. Figures 13 and 14 shows the energy consumed by the vehicle for each type of control strategy proposed. In the two figures (Figures 13 and 14), we can see that the classical DTC consumes more energy than the DTNC and the DTFC.

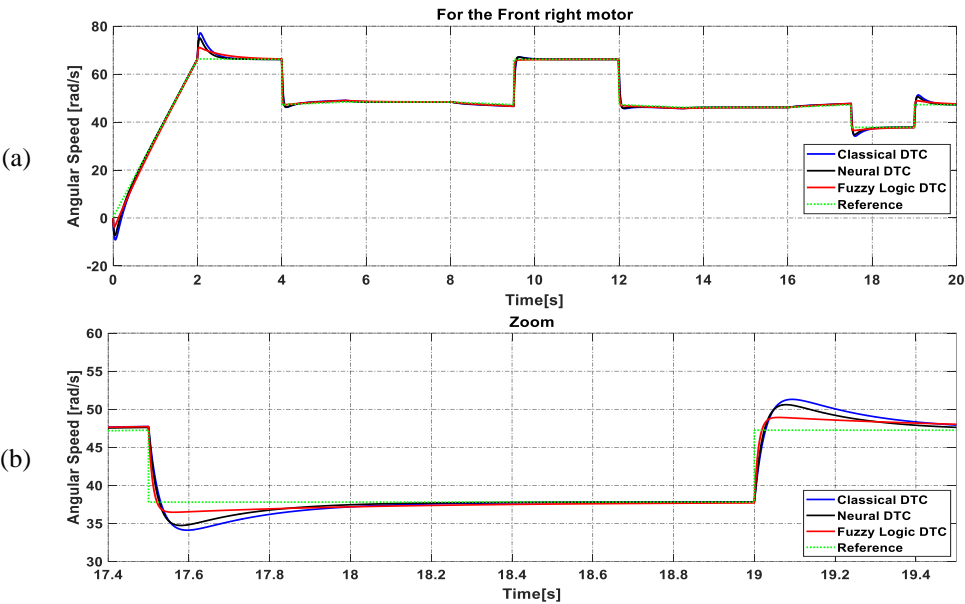


Figure 12. Right front motor angular speed (a) angular speed and (b) zoom speed

Table 3. Dynamic parameters of the speed response for each motor

Dynamic Parameters	Rising Time (Sec)			Overshoot (%)			Speed Error (%)		
	PI	FL	ANN	PI	FL	ANN	PI	FL	ANN
	0.044	0.0209	0.0356	7.27	1.56	6.89	0.07	0.02	0.07

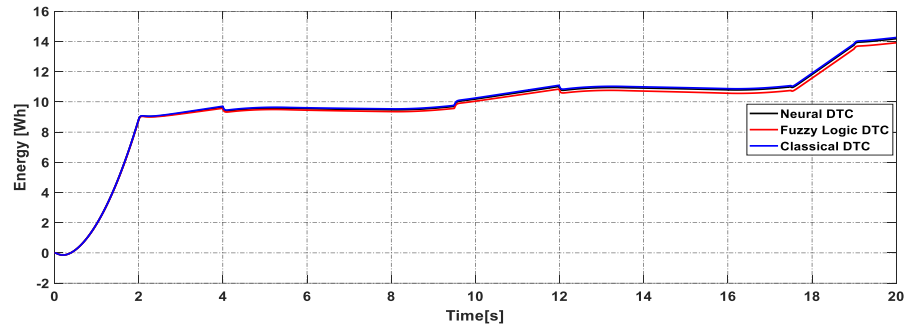


Figure 13. Electrical energy consumed by the vehicle

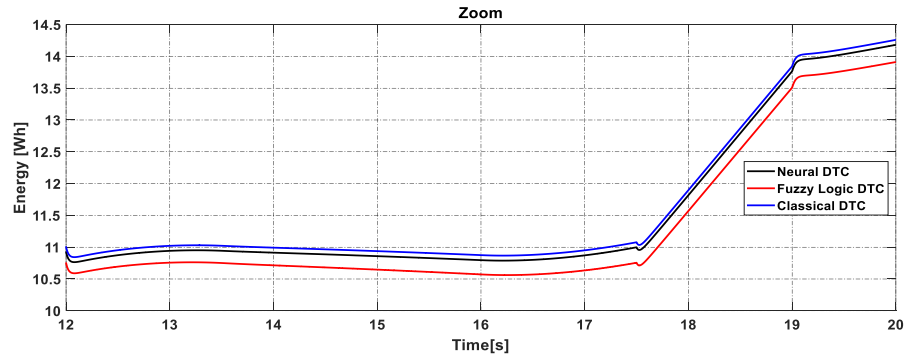


Figure 14. Zoom of the electrical energy consumed by the vehicle

To validate this model of a 4WD, 2-converter vehicle, goes through a confrontation with the WLTP driving cycle, the results of which are shown in Figure 15. This figure shows the speed of each engine of the vehicle. These speeds follow faithfully the setpoint imposed by the WLTP cycle. The proposed control system shows its robustness to the different constraints of the cycle. This ensures good stability of vehicle stability.

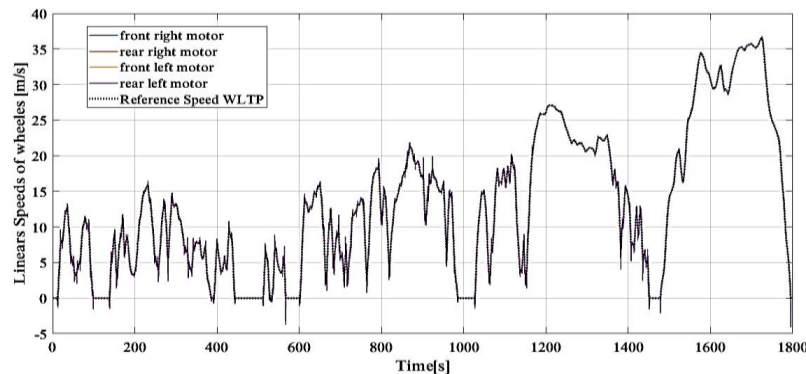


Figure 15. Speed profile with WLTP

5. CONCLUSION

In this paper, two methods of controlling multi-machine systems for electric vehicle propulsion are proposed. The results obtained show that direct torque control combined with fuzzy logic and artificial neural networks, compared with conventional control, delivers high performance in terms of speed, precision, robustness and perfect setpoint tracking despite the strong disturbances imposed by road constraints. The vehicle speed results obtained during the simulations enable a quantitative assessment of the performance of the proposed control strategies. With regard to the results and analyses previously carried out within the strict framework of the hypotheses considered (hysteresis limit range.), it is clear that the DTFC control technique presents better results (response time, static error.) than conventional DTC and DTNC. On the other hand, it can be seen that energy dissipation is a crucial factor in the quality-price ratio of an EV, as it is linked to electricity storage and therefore to battery life (charge and discharge cycle). In addition, consideration of the variation in the number of rules in DTFC and DTNC may be a future line of research to make a definitive statement concerning the comparison between these two techniques in EV modeling. All in all, the use of a twin-engine system with a single converter enables the electric vehicle to save energy. This is observed when using the WLTP driving cycle.




REFERENCES

- [1] G. C. Tripathi and R. Goswami, "Augmentation of charging infrastructure for electric vehicles growth in India," *International Journal of Electric and Hybrid Vehicles*, vol. 12, no. 1, p. 44, 2020, doi: 10.1504/ijehv.2020.10025992.
- [2] A. R. V. Babu, P. M. Kumar, and G. S. Rao, "A novel diagnostic technique to detect the failure mode operating states of an air-breathing fuel cell used in fuel cell vehicles," *International Journal of Electric and Hybrid Vehicles*, vol. 12, no. 1, pp. 32–43, 2020, doi: 10.1504/IJEHV.2020.104263.
- [3] G. Banda and S. G. Kolli, "An intelligent adaptive neural network controller for a direct torque controlled ecar propulsion system," *World Electric Vehicle Journal*, vol. 12, no. 1, 2021, doi: 10.3390/wevj12010044.
- [4] G. Ge, L. Shi, K. Yang, and D. Tan, "Research status of electronic differential control of electric vehicle driven by in-wheel motor," *International Journal of Vehicle Safety*, vol. 11, no. 4, p. 289, 2020, doi: 10.1504/ijvs.2020.10033767.
- [5] Q. Chen, S. Kang, L. Zeng, Q. Xiao, C. Zhou, and M. Wu, "PMSM control for electric vehicle based on fuzzy PI," *International Journal of Electric and Hybrid Vehicles*, vol. 12, no. 1, pp. 75–85, 2020, doi: 10.1504/IJEHV.2020.104271.
- [6] T. Isao and O. Youichi, "High-Performance Direct Torque Control of an Induction Motor," *IEEE Transactions on Industry Applications*, vol. 25, no. 2, pp. 257–264, 1989.
- [7] G. Banda and S. G. Kolli, "Comparison of ANN- and GA-based DTC eCAR," *Journal of Power Electronics*, vol. 21, no. 9, pp. 1333–1342, 2021, doi: 10.1007/s43236-021-00273-1.
- [8] G. Banda and S. G. Kolli, "Comparison of ANN- and GA-based DTC eCAR-," *Journal of Power Electronics*, vol. 21, no. 9, pp. 1333–1342, 2021, doi: 10.1007/s43236-021-00273-1.
- [9] A. Derbane, B. Tabbache, and A. Ahriche, "A fuzzy logic approach based direct torque control and five-leg voltage source inverter for electric vehicle powertrains," *Revue Roumaine des Sciences Techniques Serie Electrotechnique et Energetique*, vol. 66, no. 1, pp. 15–20, 2021.
- [10] N. El Ouanjli *et al.*, "Modern improvement techniques of direct torque control for induction motor drives-A review," *Protection and Control of Modern Power Systems*, vol. 4, no. 1, 2019, doi: 10.1186/s41601-019-0125-5.
- [11] A. Verma, B. Singh, and D. Yadav, "Investigation of ANN tuned PI speed controller of a modified DTC induction motor drive," *2014 IEEE International Conference on Power Electronics, Drives and Energy Systems, PEDES 2014*, 2014, doi: 10.1109/PEDES.2014.7042146.




- [12] X. Sun, L. Feng, K. Diao, and Z. Yang, "An Improved Direct Instantaneous Torque Control Based on Adaptive Terminal Sliding Mode for a Segmented-Rotor SRM," *IEEE Transactions on Industrial Electronics*, vol. 68, no. 11, pp. 10569–10579, 2021, doi: 10.1109/TIE.2020.3029463.
- [13] H. Aygun and M. Aktas, "A Novel DTC Method with Efficiency Improvement of IM for EV Applications," *Engineering, Technology & Applied Science Research*, vol. 8, no. 5, pp. 3456–3462, 2018, doi: 10.48084/etasr.2312.
- [14] R. Araria, K. Negadi, and F. Marignetti, "Design and Analysis of the Speed and Torque Control of IM with DTC Based ANN Strategy for Electric Vehicle Application," *TECNICA ITALIANA-Italian Journal of Engineering Science*, vol. 63, no. 2–4, pp. 181–188, 2019, doi: 10.18280/ti-ijes.632-410.
- [15] E. Esmailzadeh, G. R. Vossoughi, and A. Goodarzi, "Dynamic modeling and analysis of a four motorized wheels electric vehicle," *Vehicle System Dynamics*, vol. 35, no. 3, pp. 163–194, 2001, doi: 10.1076/vesd.35.3.163.2047.
- [16] M. Khalfaoui, K. Hartani, A. Merah, and N. Aouadj, "Development of shared steering torque system of electric vehicles in presence of driver behaviour estimation," *International Journal of Vehicle Autonomous Systems*, vol. 14, no. 1, pp. 18–39, 2018, doi: 10.1504/IJVAS.2018.093100.
- [17] M. Abe, "Fundamentals of Vehicle Dynamics," *Vehicle Handling Dynamics*, pp. 45–107, 2015, doi: 10.1016/b978-0-08-100390-9.00003-8.
- [18] J. Y. Wong, "Theory of Ground Vehicles," *Theory of Ground Vehicles*, 2022, doi: 10.1002/9781119719984.
- [19] M. Bensaid, B. Rached, M. Elharoussi, and A. Ba-Razzouk, "Multi-drive electric vehicle system control using backstepping strategy," *2020 1st International Conference on Innovative Research in Applied Science, Engineering and Technology, IRASET 2020*, 2020, doi: 10.1109/IRASET48871.2020.9092164.
- [20] T. Ahmed, H. Kada, and A. Ahmed, "New DTC strategy of multi-machines single-inverter systems for electric vehicle traction applications," *International Journal of Power Electronics and Drive Systems*, vol. 11, no. 2, pp. 641–650, 2020, doi: 10.11591/ijpeds.v11.i2.pp641-650.
- [21] N. Matéké Max, N. Yome Jean Maurice, E. Samuel, B. Laurent, and A. Biboum, "Electric Vehicle Wheel Drive Analysis Using Direct Torque Fuzzy Control Method."
- [22] M. Sekour, K. Hartani, and A. Merah, "Electric vehicle longitudinal stability control based on a new multimachine nonlinear model predictive direct torque control," *Journal of Advanced Transportation*, vol. 2017, no. 1, 2017, doi: 10.1155/2017/4125384.
- [23] K. Hartani, M. Bourahla, and Y. Miloud, "New anti-skid control for electric vehicle using behaviour model control based on energetic macroscopic representation," *Journal of Electrical Engineering*, vol. 59, no. 5, pp. 225–233, 2008.
- [24] K. Hartani, M. Khalfaoui, A. Merah, and N. Aouadj, "A Robust Wheel Slip Control Design with Radius Dynamics Observer for EV," *SAE International Journal of Vehicle Dynamics, Stability, and NVH*, vol. 2, no. 2, pp. 135–146, 2018, doi: 10.4271/10-02-02-0009.
- [25] H. B. Pacejka and E. Bakker, "The magic formula tyre model," *Vehicle System Dynamics*, vol. 21, no. sup1, pp. 1–18, 1992, doi: 10.1080/00423119208969994.
- [26] "Vehicle Dynamics and Control," *Vehicle Dynamics and Control*, 2006, doi: 10.1007/0-387-28823-6.
- [27] N. M. Max, N. Y. J. Maurice, E. Samuel, M. C. Jordan, A. Biboum, and B. Laurent, "Dtc with fuzzy logic for multi-machine systems: Traction applications," *International Journal of Power Electronics and Drive Systems*, vol. 12, no. 4, pp. 2044–2058, 2021, doi: 10.11591/ijpeds.v12.i4.pp2044-2058.
- [28] A. Nasri, B. Gasbaoui, and B. M. Fayssal, "Sliding Mode Control for Four Wheels Electric Vehicle Drive," *Procedia Technology*, vol. 22, pp. 518–526, 2016, doi: 10.1016/j.protcy.2016.01.111.
- [29] M. K. Metwaly *et al.*, "Smart integration of drive system for induction motor applications in electric vehicles," *International Journal of Power Electronics and Drive Systems*, vol. 12, no. 1, pp. 20–28, 2021, doi: 10.11591/ijpeds.v12.i1.pp20-28.

BIOGRAPHIES OF AUTHORS






Ndoumbé Matéké Max    is a lecturer and researcher at the University of Douala, Cameroon. Holder of a teacher's diploma of technical high schools' option Electrotechnics obtained in 2012 and a master's degree in Electrotechnics, Electronics, Automation and Telecommunication at the University of Douala in 2015. He obtained a Ph.D. in Engineering Sciences with a specialization in Industrial Electronics and Systems. Research interests: power conversion, high-power, variable-speed drives, electric vehicles. He can be contacted at email: mdesmax@yahoo.fr.






Njock Batake Emmanuel Eric    was born in Cameroon on November 13th, 1991. He received the Engineering degree from the National Advanced School of Engineering in the University of Yaoundé, Cameroon, in 2019, and the Master degree from the Postgraduate School for Pure and Applied Science (POSPAS) in Douala, in 2020, both in electrical engineering. He is currently working toward the Ph.D. degree at the Laboratory of Energy, Materials, Modeling and Methods of the POSPAS, in the Department of Robotics. His research interests include modeling and modern control of Electrical machine using neural and fuzzy logic control, applied to power electronics system, and electric vehicle. He can be contacted at email: e.njockbatake@gmail.com.






Nyobe Yomé Jean Maurice    was born in Yaoundé, Cameroon. He received the Diploma degree in Electrical Engineering of Advanced Teacher Training College for Technical Education from the University of Douala- (ATTCTE/ENSET), Cameroon, in 1984, and joined the University of Douala-ENSET as a lecturer where he is currently an associate Professor. He received the M.S. degree in Electrical Engineering jointly from the Ecole Normale Supérieure de Cachan, France and the Université de Paris VI, Paris, France, in 1986, and the Ph.D. degree in Electrical Engineering from the Université Montpellier II (STL), France in 1993. He is a Senior Member of Cameroon Commission for Technical Education. His area interest are resonant power conversion, high-power variable-speed drives, wind-mill/diesel twinning, and applied pedagogical science to electrical engineering. He is actually the Deputy Director of the National Higher Polytechnic School of Douala. He can be contacted at email: nyobeyome@yahoo.fr.






Mouné Cédric Jordan    was born in Douala (Cameroon) on June 1999. In 2021, he graduated with a master 2 research in Electric Energy and Robotic at the National Advanced School of Engineering of Douala, where he has since pursued a postgraduate study. Field of study: electrical drives systems and power electronics. He can be contacted at email: mouneced157@gmail.com.






Manyol Moise    holds a Diploma of High School Teacher of Technical Education option Electrical Engineering obtained in 2010 at the University of Douala in Cameroon, and a Master's degree in Electronics, Electrical Engineering Automation obtained in 2014 in the Faculty of Science of the University of Ngaoundere in Cameroon. He is currently preparing a PhD thesis in Artificial Intelligence and Fault Prediction of Power Transformers at the Energy, Materials, Modelling and Methods (E3M) Laboratory of the National Polytechnic School of the University of Douala since 2020. His research interests include power transformer maintenance, knowledge extraction from maintenance data and data analysis techniques. He can be contacted at email: moisemany@yahoo.fr.



Olong Georges    received his Diploma in Electrical Engineering in 2004 from the Advanced Teacher's Training College for Technical Education (ATTCTE), Douala, Cameroon in 2016 obtained a Master Sc. in Electrical Engineering and Robotics from the University of Douala, where he is currently pursuing a PhD in Electrical Engineering from the National Higher Polytechnic School, University of Douala, Cameroon since 2020 at the Energy Modelling Material and Methods (E3M) Laboratory of the University of Douala. His area of research is a technical and economic analysis of Cameroon's energy potential. He can be contacted at email: geobilong@gmail.com.



Alain Biboum    Biboum Alain Christian holds a PhD in Energy from Ege University, Izmir Turkey. He is a university lecturer and works for the Ministry of Higher Education of Cameroon, mainly at the National Polytechnic School of the University of Yaoundé 1. His areas of competence and expertise are: industrial engineering, operations management, optimization of energy systems, advanced thermoeconomics, energy production and planning, energy regulation framework and policies for government, thermal power plants, hydrogen production, liquefaction and storage, hybrid thermal power plants for industrial processes. He can be contacted at email: alain.biboum@univ-yaounde1.cm.